This is the accepted manuscript made available via CHORUS. The article has been published as:

Magnetic Resonance Imaging by Synergistic Diffusion-Diffraction Patterns

Noam Shemesh, Carl-Fredrik Westin, and Yoram Cohen

Magnetic Resonance Imaging by synergistic diffusion-diffractions

Noam Shemesh[*] and Yoram Cohen[*]

School of Chemistry, The Raymond and Beverly Sackler Faculty of Exact Sciences, Tel Aviv University.

*Corresponding authors:

1. Yoram Cohen,

School of Chemistry,

The Sackler Faculty of Exact Sciences,

Tel Aviv University, Ramat Aviv,

Tel Aviv 69978, Israel.

Tel: 972-3-6407232. Fax: 972-3-6407469

E-mail: ycohen@post.tau.ac.il

2. Noam Shemesh,

School of Chemistry,

The Sackler Faculty of Exact Sciences,

Tel Aviv University, Ramat Aviv,

Tel Aviv 69978, Israel.

Tel: 972-3-6406949. Fax: 972-3-6407469

E-mail: nshemesh@gmail.com

One sentence summary: MRI by synergistic diffusion-diffraction patterns

Abstract

Inferring on the geometry of an object from its frequency spectrum is a highly appealing concept since it would allow one to image the object noninvasively or from a distance, or as famously put by Kac in 1966: "can one hear the shape of a drum?". The answer was no, since different geometries may produce identical frequency spectra. The problem translates directly to Nuclear Magnetic Resonance (NMR) of porous systems, where the shape of the drum is represented by the pore density function that bears all the information on the collective pore microstructure. Insofar, similarly to the answer to Kac's question, conventional MR methods could not report on the pore density function directly, since they inherently detect the pore autocorrelation function (ACF), which can be similar for very different pore geometries. Here, we report on direct detection of the pore density function for the first time using unique synergistic diffusion-diffraction patterns arising from two diffusion MR methodologies. The pore spectrum is directly detected, retaining all fine details on the collective pore morphology. This in fact results in a unique imaging mechanism that provides substantially higher spatial resolution compared to conventional MRI. We conclude that using this synergistic approach for MR imaging, one can "hear the shape of a drum", i.e. one can directly detect the pore density function from its frequency spectrum.

Text

Opaque porous systems are highly diverse and are prevalent in many important areas of research. Porous materials [1-3], heterogeneous catalysts [4], rocks that contain oil reservoirs [5], and even biological tissues [6] are but a few examples. Characterizing the morphology of the constituent pores is of paramount importance in such systems since the pore structure can determine physical or even biological properties of the medium. In 1966, Kac famously posed his question: "can one hear the shape of the drum?" [7], alluding to the possibility of inferring on the structure of an object from its frequency spectrum, i.e., noninvasively or from a distance. Kac's question, which was negatively answered [8] due to similar frequency responses of different geometries, can be translated to MR of porous media, where the collective pore microstructure represents the "drum" and the MR signal represents the frequency response; insofar, conventional MR methods could not detect the direct frequency spectrum of the pore microstructure, since the autocorrelation function (ACF) of the pore microstructure is inherently detected [1, 9], resulting in a loss of fine details on the pore morphology *(vide-infra)* and adhering to the negative answer to Kac's question.

Magnetic Resonance Imaging (MRI) [10] has indeed become the most important noninvasive imaging modality in biological and medical applications since it is completely noninvasive, safe, multi-modal, and offers excellent penetration. Conventional MRI utilizes magnetic field gradients to image the spin density function (SDF) which describes the spatial distribution of spins within the specimen, i.e. a map of MR-responsive nuclear spin concentration as function of position is obtained. Spatial encoding in conventional MRI is achieved by applying imaging gradients that impart spatial frequency dependencies, which upon Fourier Transform (FT) of the MR signal directly yield the SDF [10]. However, an inherent limitation ensues: as the spatial resolution is enhanced, fewer spins contribute to the signal in each voxel, leading to deterioration of the signal-to-noise ratio (SNR) and thus posing a practical constraint on the

available resolution in MRI, especially in spin-deprived systems such as bulk hosts with small-scale pore domains.

In many systems, and especially those that are related to porous systems, the actual position of spins is not of particular interest; on the other hand, the structural properties such as size and shape of the constituent pores are of paramount importance. The use of restricted diffusion as an endogenous reporter has been previously proposed as a probe for pore microstructure [1], and previous studies were able to image the autocorrelation function of the pore space, analogous to the Patterson functions obtained in X-ray diffraction [1, 2]; however, fine details on pore morphology are obscured since it is the phase-insensitive power spectrum of the collective pore microstructure that is detected. In this PRL, we demonstrate for the first time that the collective pore microstructure spectrum can be directly obtained from unique synergistic diffusion-diffraction patterns arising from two diffusion NMR spectroscopy experiments. An MR image of the collective pore microstructure is directly obtained sans traditional "imaging" gradients, i.e., via a starkly different imaging mechanism compared to conventional MRI. Advantageously, these experiments are spectroscopic in nature, i.e. the MR signal originates from the entire specimen; thus, no fundamental resolution limit exists, excluding diffusion gradient amplitude.

Restricted diffusion occurs when fluid is enclosed within a pore domain whose boundaries impose physical restriction on the diffusing molecules. Given sufficient time to probe the pore boundaries, the molecules fully experience the restriction effects and can therefore be used as unique endogenous reporters for the pore microstructure [11]. The MR signal can be sensitized to diffusion processes via application of a single diffusion weighting gradient vector, **G** comprised of two opposite "sense" gradient pulses that are separated by the diffusion time, Δ [12]. The conventional single-Pulsed-Gradient-Spin-Echo (s-PGSE) MR methodology for measuring diffusion effects [12] is shown in Figure S1A. The 90° and 180° RF pulses serve as excitation and refocusing pulses, respectively. The first diffusion-weighting gradient pulse winds a magnetization helix which induces a spatially-dependent phase shift, and then the spins are allowed to diffuse during Δ. The second gradient pulse acts to unwind the magnetization helix

and to refocus the previously acquired phase shift. Stationary spins will indeed acquire zero net phase; however, mobile spins will experience a mismatch between the phases acquired during each gradient pulse, and will therefore acquire a finite net phase. Consequently, the MR signal amplitude will attenuate compared to the signal in the absence of gradients, solely due to mobile diffusing spins.

The diffusion process can be described statistically by the diffusion propagator $P(r_0, r_1, \Delta)$, which describes the probability for a spin originating at r_0 to arrive at r_1 during the diffusion time Δ. Taking into account the phase that would accumulate from every possible displacement $R = r_1 - r_0$ and by integrating over all initial and final positions, the diffusion MR attenuation for s-PGSE sequences, $E^{sPGSE}(q, \Delta)$, can be therefore written completely generally (assuming that gradient durations are short (the so-called short-gradient-pulse (SGP) approximation) [1, 9]:

$$E^{sPGSE}(q, \Delta) = \int \int \rho(r_0) P(r_0, r_1, \Delta) e^{i2\pi q \cdot (r_1 - r_0)} dr_0 dr_1 \tag{1}$$

The complex exponential term describes the phase accumulated, $q = \frac{1}{2\pi} \gamma \delta G$ is the reciprocal space wavevector, γ is the gyromagnetic ratio, δ is the gradient pulse duration, and $\rho(r_0)$ is the initial SDF. When fully restricted diffusion is considered, $\rho(r)$ in fact represents the pore density function, which is taken as the reciprocal of the pore volume within the pore boundaries and zero elsewhere. Note that in this case, the definition of $\rho(r)$ departs from the definition of the SDF as it is not the positions of pores within the specimen that is described; rather, the collective microstructural properties are considered [1, 2].

In fact, $\rho(r)$ is a 1-dimensional projection image of the pore space, bearing all of the information on the pore microstructure. Figure 1A shows two different representative pores of rectangular and cylindrical geometry, both with a restricting length scale of $L = 2r = 22.5 \, \mu m$, placed along the z-direction. For rectangular and cylindrical pores, the corresponding pore density functions $\rho(r)$ are the box-function, and the cylinder function, respectively [9] (Figure 1B).

To reach the fully restricted diffusion regime, the diffusion period must be long ($\Delta_{\to\infty}$), such that all spins sample the pore boundaries and diffusion becomes independent of the initial position. Then, $P(\mathbf{r_0}, \mathbf{r_1}, \infty)$ simply reduces to $\rho(\mathbf{r_1})$, the final spin density function, which is in fact identical to $\rho(\mathbf{r_0})$ and in general to $\rho(\mathbf{r})$, the pore density function. It is then straightforward to show that the s-PGSE MR signal decay due to diffusion is in fact the power spectrum of the pore space [1, 9]:

$$E^{sPGSE}(\mathbf{q}, \Delta_{\to\infty}) = \int \rho(\mathbf{r_0})e^{-i2\pi\mathbf{q}\cdot\mathbf{r_0}}d\mathbf{r_0} \int \rho(\mathbf{r_1})e^{i2\pi\mathbf{q}\cdot\mathbf{r_1}}d\mathbf{r_1} \qquad (2)$$

$$E^{sPGSE}(\mathbf{q}, \Delta_{\to\infty}) = |\tilde{\rho}(\mathbf{q})|^2 \qquad (3)$$

where the structure function $\tilde{\rho}(\mathbf{q})$ is simply the FT of $\rho(\mathbf{r})$. The structure functions $\tilde{\rho}(\mathbf{q})$ for rectangular pores and cylindrical pores are $\tilde{\rho}(\mathbf{q}) = sinc(\pi q L)$ and $\tilde{\rho}(\mathbf{q}) = \frac{J_1(2\pi qr)}{\pi qr}$, respectively (Figure 1C), where $J_1(x)$ is the first order Bessel function. Detection of the structure function would be highly beneficial since upon FT it would yield a direct 1-dimensional image projection of the pore space. However, Equation 3 precludes direct detection of $\tilde{\rho}(\mathbf{q})$; rather, it is the power spectrum that is inherently detected. Fundamentally, the power spectrum $|\tilde{\rho}(\mathbf{q})|^2$ is in fact the FT of the averaged diffusion displacement propagator $\bar{P}(\mathbf{R}, \infty) = \int \rho(\mathbf{r_0})P(\mathbf{r_0}, \mathbf{r_0} + \mathbf{R}, \infty)d\mathbf{r_0} = \int \rho(\mathbf{r_0})\rho(\mathbf{r_0} + \mathbf{R})d\mathbf{r_0}$ which for fully restricted diffusion is in fact the ACF of the pore space (Figure 1D). The s-PGSE MR signal acquired as a function of the q-value therefore exhibits constantly positive diffusion-diffraction patterns (Figure 1E) which are the Fourier Transform (FT) of the pore ACF. An 'image' of the ACF can therefore be obtained from the diffusion-diffraction patterns without actually performing conventional frequency-encoded MR imaging that entails the resolution limitations outlined above [1, 2, 9]. While useful information can be inferred from the diffusion-diffraction patterns or the ACF 'image' in diverse systems ranging from porous materials [1, 2] to electric charge diffusing in a conductor [13], fine details on the pore geometry are obscured or lost (Figure 1D) since the ACFs of different geometries are quite similar.

Recently, an extension of s-PGSE MR, namely double-PGSE (d-PGSE) MR [14] has been emerging as a novel means for obtaining microstructural information in highly heterogeneous systems [15-17]. Figure S1B, shows the d-PGSE sequence at the zero-mixing time regime, with its two independent gradient vectors $\mathbf{G_1}$ and $\mathbf{G_2}$ that span the diffusion periods Δ_1 and Δ_2. A derivation similar to the one outlined above can be used to assess the signal decay in d-PGSE MR when restricted diffusion occurs [18]; briefly, at the zero mixing time regime, we may write the signal decay in terms of the probability to diffuse from $\mathbf{r_0}$ to $\mathbf{r_1}$ during Δ_1 and from $\mathbf{r_1}$ to $\mathbf{r_2}$ during Δ_2:

$$E^{dPGSE}(\mathbf{q_1}, \mathbf{q_2}, t_m = 0, \Delta_1, \Delta_2) =$$

$$\int \rho(\mathbf{r_0})e^{-i2\pi \mathbf{q_1}\cdot \mathbf{r_0}}d\mathbf{r_0} \int \rho(\mathbf{r_1})P(\mathbf{r_0}, \mathbf{r_1}, \Delta_1)e^{i2\pi(\mathbf{q_1}+\mathbf{q_2})\cdot \mathbf{r_1}}d\mathbf{r_1} \int \rho(\mathbf{r_2})P(\mathbf{r_1}, \mathbf{r_2}, \Delta_2)e^{-i2\pi \mathbf{q_2}\cdot \mathbf{r_2}}d\mathbf{r_2} \tag{4}$$

where $\mathbf{q_i} = \frac{1}{2\pi}\gamma\delta_i\mathbf{G_i}$. We are interested in the long diffusion limit where $\Delta_1 = \Delta_2 \equiv \Delta_{\rightarrow\infty}$, and in identical wavevectors $\mathbf{q_1} = \mathbf{q_2} \equiv \mathbf{q}$; recalling that $P(\mathbf{r_i}, \mathbf{r_{i+1}}, \infty)$ simply reduces to $\rho(\mathbf{r_{i+1}})$ for fully restricted diffusion, Eq. 4 can be rewritten as

$$E^{dPGSE}(\mathbf{q}, \Delta_{\rightarrow\infty}) = \int \rho(\mathbf{r_0})e^{-i2\pi \mathbf{q}\cdot \mathbf{r_0}}d\mathbf{r_0} \int \rho(\mathbf{r_1})e^{i4\pi \mathbf{q}\cdot \mathbf{r_1}}d\mathbf{r_1} \int \rho(\mathbf{r_2})e^{-i2\pi \mathbf{q_2}\cdot \mathbf{r_2}}d\mathbf{r_2} \tag{5}$$

The first and last terms are simply the pore structure function $\tilde{\rho}(\mathbf{q})$, while the middle term is its conjugate with doubled frequency. Therefore, under the SGP approximation, the d-PGSE MR signal is simply:

$$E^{dPGSE}(\mathbf{q}, \Delta_{\rightarrow\infty}) = \tilde{\rho}(\mathbf{q})^2\tilde{\rho}^*(2\mathbf{q}) \tag{6}$$

where $\tilde{\rho}^*(\mathbf{q})=\tilde{\rho}(-\mathbf{q})$. Note that the latter non-squared term in Eq. 6 suggests that d-PGSE MR experiments should exhibit a unique "negative-diffraction" pattern that was very recently observed experimentally for the first time [15, 16, 19].

While neither individual methodology is capable of providing a direct image of the pore microstructure, synergistic application of both methods may indeed provide the so far unattainable information. When Equations 6 and 3 are divided, the synergistic signal decay, $N(\mathbf{q})$, is obtained:

$$N(\boldsymbol{q}) = \frac{E^{dPGSE}(\boldsymbol{q}, \Delta_{\to\infty})}{E^{sPGSE}(\boldsymbol{q}, \Delta_{\to\infty})} = \frac{\tilde{\rho}(\boldsymbol{q})^2 \tilde{\rho}^*(2\boldsymbol{q})}{|\tilde{\rho}(\boldsymbol{q})|^2} = \tilde{\rho}^*(2\boldsymbol{q}) \tag{7}$$

Equation 7 is truly remarkable since it suggests that by synergistically applying the two measurements, one would obtain a phase-sensitive modulated diffusion-diffraction pattern of the structure function, $\tilde{\rho}(\boldsymbol{q})$, which would directly yield a 1-dimensional projection image of the pore microstructure upon FT (the factor of two in Eq. 7 is simply a scaling factor). Note that this image would only be limited in resolution by the q-value, i.e. by the amplitude of the diffusion-weighting gradients; furthermore, as the signal is acquired in spectroscopic mode, all spins in the specimen contribute to the signal, i.e. the inherent resolution limitation imposed by gradients in conventional MRI is obviated.

To test whether indeed this novel approach could provide an image of the microstructure, we performed both s-PGSE and d-PGSE NMR spectroscopy experiments on an ensemble of water-filled cylindrical microcapillaries (the nominal inner diameter was 23±1 μm) that were coherently aligned with their principal axis pointing at the z-direction, the direction of the external 8.4 T magnetic field (see Supplementary Material for materials and methods). Experiments were performed in the plane perpendicular to the principal axis of the microcapillaries, and with diffusion times of 110 ms, sufficiently long to reach the fully restricted diffusion regime [19-21] . The maximum gradient strength used was 0.8 T/m.

Figures 2A-C show the signal decay in the s-PGSE and d-PGSE MR spectroscopy experiments. The s-PGSE MR experiments exhibits constantly positive diffusion-diffraction patterns. The d-PGSE MR signal exhibits the zero-crossings and consequently, the negative-diffraction patterns, as predicted by Eq. 6. Figure 2D shows $N(\boldsymbol{q})$ data, obtained by dividing the experimental data in the two individual experiments. Indeed, the synergistic signal decay $N(\boldsymbol{q})$ appears remarkably similar to the form of $\tilde{\rho}(\boldsymbol{q})$ shown in Figure 1C. Figure 2E shows the FT of $N(\boldsymbol{q})$. Indeed, a 1-dimensional projection of the cylindrical pore microstructure was directly obtained, i.e. an image of the pore density function, $\rho(\boldsymbol{r})$, was directly obtained for the first time. The pore dimensions are in excellent agreement with the nominal

inner diameter, with the apparent radius being ~11 μm. Figure 2F shows the FT of the s-PGSE MR $E(\boldsymbol{q})$ data, for comparison. As expected, a triangular ACF of the pore space is obtained. The dimension of the pores can in fact be inferred from the base of the triangle since it describes the maximum displacement available in the system. Here, the maximum displacement is ~21.75 μm, in very good agreement with the nominal pore diameter. However, inherently, the fine details of the pore structure are lost, and as shown in Figure 1D, very similar results would be obtained for pores having different microstructure.

The structure function $\tilde{\rho}(\boldsymbol{q})$ for cylindrical pores of radius r is $\tilde{\rho}(\boldsymbol{q}) = \frac{J_1(2\pi qr)}{\pi qr}$. We therefore fitted the $N(\boldsymbol{q})$ data to this function. The pore diameter that was obtained was 22.5±0.6 μm, in excellent agreement with the nominal inner diameter of the pores, i.e. 23±1 μm (Figure 3). We then attempted to create a two-dimensional MR image based on $\rho(\boldsymbol{r})$ using back-projection of the $N(\boldsymbol{q})$ data (extrapolated to encompass twice as many zero-crossings as in the original data, to offer smoother images), via an inverse Radon transform (assuming cylindrical symmetry). The 2-dimensional image of the pore microstructure in the plane perpendicular to the principal axis of the pores is shown in Figure 4A. Note that this is an MRI image of the pore microstructure that was obtained without application of traditional imaging gradients. Figure 4B shows the 2-dimensional back-projection of the ACF obtained from the FT of similarly extrapolated $E(\boldsymbol{q})$ data from s-PGSE MR experiments. As shown previously, the fine details of the pore microstructure are absent due to the lack of zero-crossings, i.e. phase information, in the original $E(\boldsymbol{q})$ data; however, the details on the maximum displacement can be inferred. In the images shown in Figure 4, the in-plane resolution, which depends only on the maximum q-value used, is 1.84x1.84 (μm)^2. Acquiring the $N(\boldsymbol{q})$ data up to higher q-values using stronger gradients would yield even much higher resolution.

The findings reported here provide the first experimental evidence that a direct MR image of the collective pore microstructure can be obtained by synergistic application of the d-PGSE and s-PGSE diffusion MR methodologies. The unique synergistic diffraction patterns shown here directly afforded the

pore spectrum, which is elusive for conventional MR imaging methods. Furthermore, since all spins in the small pore domains contribute to the MR signal, an image of the pore density function can be obtained at very high resolution.

A very recent study suggested that the pore density function can even be obtained in s-PFG MR, if the temporal symmetry of the gradients is broken [22]. Another MR imaging technique that can achieve extremely high resolution is MR force microscopy (MRFM) [23], which necessitates highly sophisticated instruments, vacuum, and very cold temperature; however, the method presented here is general and can indeed be used in any conventional NMR or MRI scanners. We note by passing that the PGSE sequences can be weighted by relaxation by changing the echo times, and thus such images can even offer multi-modality. The only limitations on resolution are the gradient amplitude and the fulfillment of the short gradient pulse approximation. However, with the recent developments in gradient coil technologies (gradient coils capable of producing up to 45 T/m were recently reported [24]) and since spins trapped in small pores can be cooled such that they will diffuse negligibly during the gradient pulses [25], direct and completely noninvasive sub-micrometer MR imaging of ordered structures, perhaps even on the nanoscale, should be attainable by this methodology. It should be noted, however, that application of this methodology in-vivo would be very difficult considering the very strong gradients needed to image small pores and since diffraction patterns in s-PFG MR may be lost when large distributions are present [15, 16]. Nevertheless, the proposed methodology may be used to characterize many other types of porous systems for which gradient amplitude is not a significant constraint. Additionally, for some distributions, it may even be possible to tweak the diffusion periods such that components of the distribution are emphasized [19, 26].

Finally, we note that with analogy to Kac's famous question, we have shown here experimentally for the first time that in NMR, one can in fact obtain the pore structure noninvasively directly from its frequency spectrum.

References

1. P. T. Callaghan et al., *Nature* **351**, 467 (1991).

2. G. A. Barrall, L. Frydman, and G. C. Chingas, *Science* **255**, 714 (1992).

3. R. Valiullin et al., *Nature* **443**, 965 (2006).

4. V. Kukla et al., *Science* **272**, 702 (1996).

5. Y. Q. Song, S. G. Ryu, and P. N. Sen, *Nature* **406**, 178 (2000).

6. D. Le Bihan, *Nat. Rev. Neurosci.* **4**, 469 (2003).

7. M. Kac, *Am. Math. Monthly* **73**, 1 (1966).

8. C. Gordon, D. L. Webb, and S. Wolpert, *Bull. Am. Math. Soc.* **27**, 134 (1992).

9. W. S. Price, *Concepts Magn. Reson.* **9**, 299 (1997).

10. P. C. Lauterbur, *Nature* **242**, 190 (1973).

11. P. P. Mitra, P. N. Sen, L. M. Schwartz, and P. Ledoussal, *Phys. Rev. Lett.* **68**, 3555 (1992).

12. E. O. Stejskal and J. E. Tanner, *J. Chem. Phys.* **42**, 288 (1965).

13. A. Feintuch, A. Grayevsky, N. Kaplan, and E. Dormann, *Phys. Rev. Lett.* **92**, 156803 (2004).

14. D. G. Cory, A. N. Garroway, and J. B. Miller, *Polymer Preprints* **31**, 149 (1990).

15. N. Shemesh et al., *J. Chem. Phys.* **133**, 044705 (2010).

16. N. Shemesh, E. Özarslan, P. J. Basser, and Y. Cohen, *J. Chem. Phys.* **132**, 034703 (2010).

17. N. Shemesh, T. Adiri, and Y. Cohen, *J. Am. Chem. Soc.* **133**, 6028 (2011).

18. E. Özarslan and P. J. Basser, *J. Magn. Reson.* **188**, 285 (2007).

19. N. Shemesh and Y. Cohen, *J. Magn. Reson.* **195**, 153 (2008).

20. L. Avram et al., *NMR Biomed.* **21**, 888 (2008).

21. A. Bar-Shir et al., *J. Magn. Reson.* **194**, 230 (2008).

22. F. B. Laun, T. A. Kuder, W. Semmler, and B. Stieltjes, *Phys. Rev. Lett.* **107** 2011).

23. C. L. Degen et al., *Proc. Nat. Acad. Sci. U.S.A.* **106**, 1313 (2009).

24. H. H. Ong et al., *Neuroimage* **40**, 1619 (2008).

25. F. Stallmach et al., *J. Am. Chem. Soc.* **122**, 9237 (2000).

26. I. Drobnjak, B. Siow, and D. C. Alexander, *J. Magn. Reson.* **206**, 41 (2010).
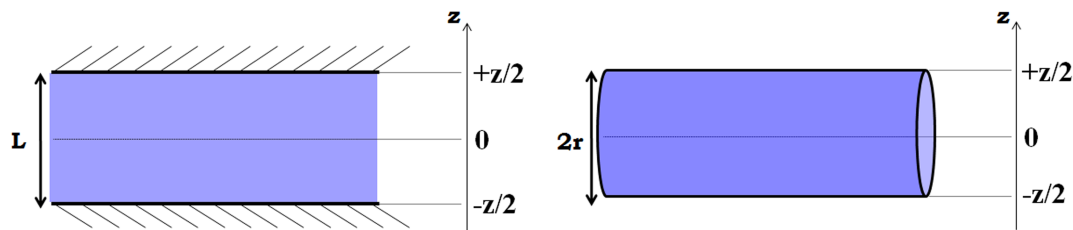
Figure Captions

Figure 1. (A) Two different representative pores having similar dimensions but different shapes. **(B)** The pore density function, $\rho(\mathbf{r})$, for each geometry. Note that the probability of finding spins outside the pore boundaries is zero. **(C)** The structure functions, $\tilde{\rho}(\mathbf{q})$, which are obtained by FT of $\rho(\mathbf{r})$. Note that these represent the pore spectrum. **(D)** The averaged displacement propagator $\bar{P}(\mathbf{R}, \infty)$ for the pores, which for fully restricted diffusion are the pore autocorrelation functions (ACFs). **(E)** The power spectra of the pores, $|\tilde{\rho}(\mathbf{q})|^2$, which are obtained by FT of $\bar{P}(\mathbf{R}, \infty)$. Note that the power spectra are inherently detected in s-PGSE MR experiments (Equation 3).

Figure 2. (A) Raw data for both s- and d-PGSE MR experiments. **(B)** Enhancement of box in (A). **(C)** Enhancement of box in (B), showing the zero-crossings more clearly. **(D)** The $N(\mathbf{q})$ data, obtained by division of the two raw data signal decays according to Equation 7. **(E)** The FT of $N(\mathbf{q})$, clearly yields $\rho(\mathbf{r})$, the pore density function. **(F)** The FT of $E(\mathbf{q})$ for s-PGSE MR data; the expected triangular function is observed, which does not contain direct information on the pore shape. The divided data suffers from artifacts near some of the zero-crossings due to division of noise; in these cases the points were extrapolated and replaced. For s-PGSE MR, $\Delta/\delta=110/4$ ms, for d-PGSE MR, $\Delta_1=\Delta_2=110$ ms, $\delta_1=\delta_2=\delta_3=4$ ms.
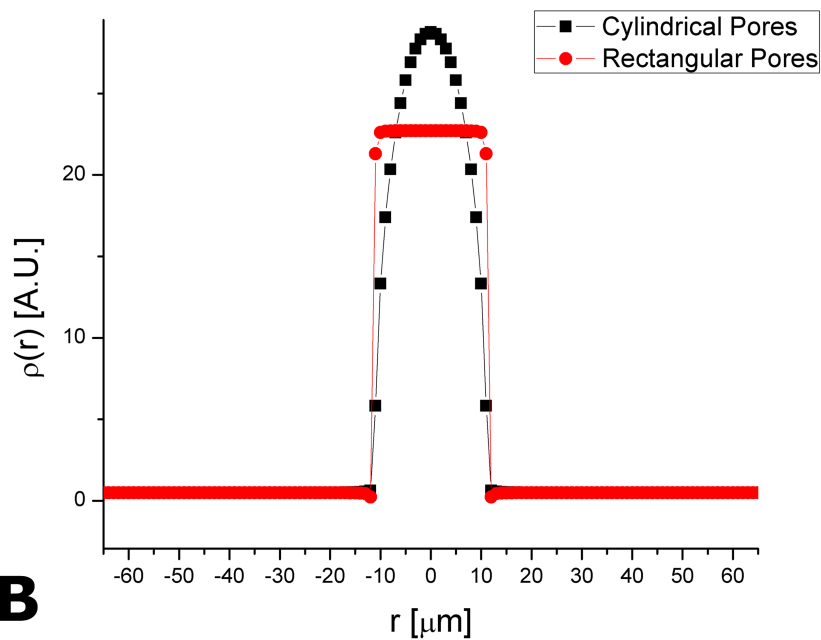
Figure 3. Theoretical fit of the experimental $N(\mathbf{q})$. The size extracted was 22.5±0.6 μm, in very good agreement with the nominal inner diameter of the pores. This dataset was used to produce the image shown in Figure 4A.

Figure 4. (A) Two dimensional back-projection of the pore density function. **(B)** Two dimensional back-projection of the pore ACF. The 1-dimensional projections of each function are shown in the insets. Note that an exact MR image of the collective pore microstructure is obtained in (A), while in (B), an image of
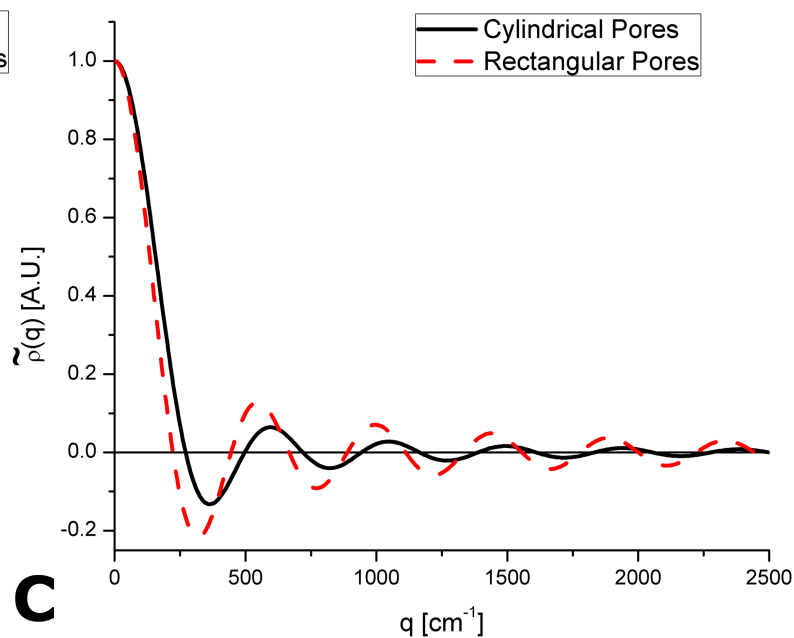
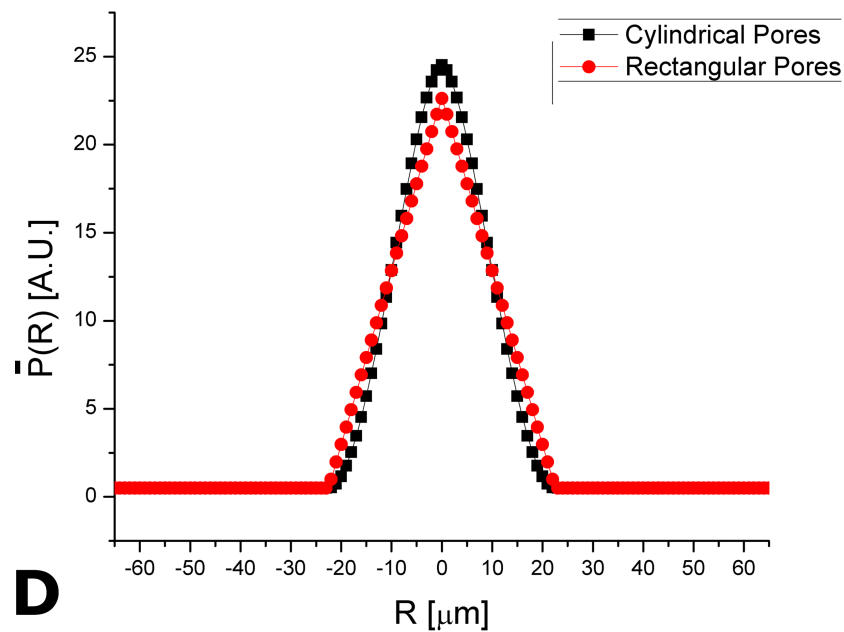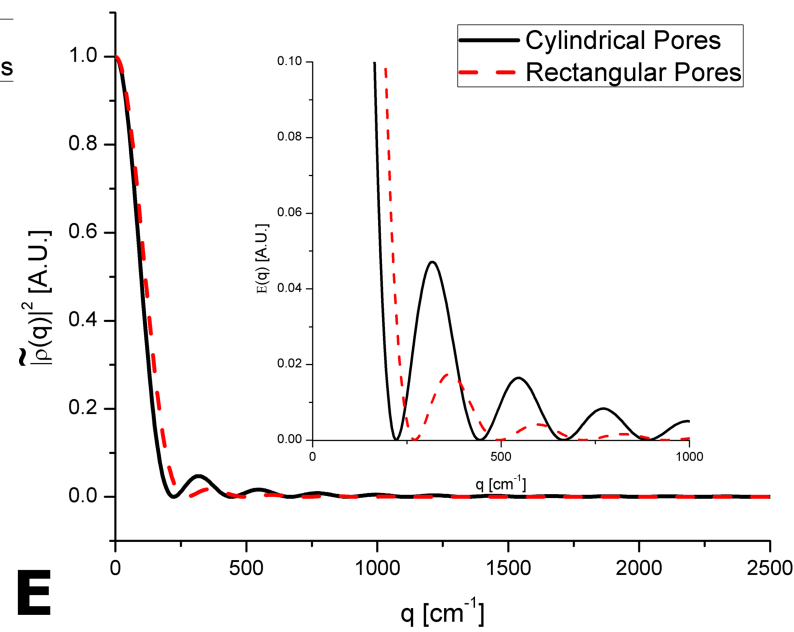the ACF is obtained. Clearly, the image of the cylinder cross-section is obtained only in (A). The in-plane resolution is ~1.8 µm.